Polyacrylamide co-N,N'-methylene bisacrylamide monoliths for high peak capacity HILIC-HRMS of intact proteins at low TFA content

Marta Passamonti[1,2*], Chiem de Roos[1], Peter J. Schoenmakers[1,2], Andrea F.G. Gargano[1,2*]

[1] Van't Hoff Institute for Molecular Sciences, University of Amsterdam, Amsterdam, The Netherlands.
[2] Centre for Analytical Sciences Amsterdam, Science Park 904, 1098 XH Amsterdam, The Netherlands.

KEYWORDS: acrylamide-based monolith, HILIC-HRMS, low TFA

ABSTRACT
In this study, we optimized a polymerization mixture to synthesize polyacrylamide-co-N,N'-methylene bisacrylamide monolithic stationary phases for hydrophilic-interaction chromatography (HILIC) of intact proteins. Thermal polymerization was performed, and the effects of varying the amount of crosslinker and the porogen composition on the separation performance of the resulting columns were studied.
The homogeneity of the structure and the different porosities were examined through scanning electron microscopy. Further characterization of the monolithic structure revealed a permeable (K_f between 2.5×10^{-15} and 1.40×10^{-13} m^2) and polar stationary phase suitable for HILIC. The HILIC separation performance of the different columns was assessed using gradient separation of a sample containing four intact proteins, with the best performing stationary phase exhibiting a peak capacity of 51 in a gradient of 25 min.
Polyacrylamide-based materials were compared with a silica-based particulate amide phase (2.7 µm core-shell particles). The monolith has no residual silanol sites and, therefore, fewer sites for ion-exchange interactions with proteins. Thus, it required lower concentrations of ion-pair reagent in HILIC of intact proteins. When using 0.1% of trifluoroacetic acid (TFA) the peak capacities of the two columns were similar (31 and 36 for the monolithic and packed column, respectively). However, when decreasing the concentration of TFA to 0.005%, the monolithic column maintained its separation performance and selectivity (peak capacity 26), whereas the packed column showed greatly reduced performance (peak capacity 7), lower selectivity, and inability to elute all four reference proteins. Finally, using a mobile phase containing 0.1% formic acid and 0.005% TFA the HILIC separation on the monolithic column was successfully hyphenated with high-resolution mass spectrometry. Detection sensitivity for protein and glycoproteins was increased and the amount of adducts formed was decreased in comparison with separations performed at 0.1% TFA.

INTRODUCTION
Monolithic stationary phases are single porous pieces of stationary phase obtained through thermal- or photo-polymerization of a mixture consisting of monomer, crosslinker, porogens and initiator. These stationary phases have been extensively investigated, because of their inherent high permeability, low resistance to mass transfer, fast and simple preparation in small formats[1–5] and a plethora of possible chemistrles and retention mechanisms.
In the mid 1990s, the first acrylamide-based monoliths were developed. Hjertén and co-workers prepared acrylamide monolithic stationary phases based on a protocol that involved the dispersion of polar monomers and crosslinkers in aqueous solutions. They obtained what they called compressible beads for LC separations.[6–8] Later, this protocol was optimized by the group of Freitag, who added dymethylformamide (DMF) as a porogen to harden the monolithic structure in capillaries used for electrochromatography applications.[9] In 1997 Xie et al. studied an alternative approach to generate more rigid materials, co-polymerizing acrylamide and methylene bisacrylamide (MbA) in dimethyl sulfoxide (DMSO) and 2-heptanol as organic solvents.[10] Materials with pore size up to 1000 nm were prepared by adjusting the synthesis conditions. No application of these materials for chromatographic purposes was reported. However, similar polymerization mixtures were later used for the production of immobilized enzyme reactors[11] and capillary electrochromatography[12] columns.

To the best of our knowledge the first applications of hydrophilic interaction chromatography (HILIC) to the study of intact proteins involved the separation of histone proteins on a weak-cation-exchange column[13–15] and later the separation of membrane proteins.[16,17] Zhang [18], Pedrali[19], Lauber[20] and Periat[21] et al. discussed the unique selectivity of HILIC in the separation of glycoforms of sub-unit and intact glycoproteins. These results have drawn attention to the use of HILIC-MS, with recent applications reporting high-resolution separations of neo-glycoproteins[22], biopharmaceuticals[23–26], biotechnological products[27] and serum immunoglobins[28]. For these proteins, HILIC resolved proteoforms that would co-elute in RPLC.

The majority of the separations of intact proteins and subunits by HILIC use silica particles with amide selectors and mobile phases based on acetonitrile, water and acidic ion-pairs, such as trifluoroacetic acid (TFA). Negatively charged ion-pair reagents are thought to neutralize the polar basic groups present in proteins, improving peak shapes and increasing the contribution of neutral polar groups, such as glycans, to retention. However, TFA and other ion-pair reagents greatly reduce MS sensitivity and can lead to gas-phase ion adducts, which complicate the mass spectra.[29]
The residual acidity of silica based materials (free silanols) is thought to be a source of non-glycan-specific ion-exchange interactions and, therefore, increases the need for ion-pair reagents in the mobile phase to enhance the separation efficiency and reduce peak tailing for glycoforms. To reduce the amount of TFA used in HILIC separations of proteins Wirth and co-workers[18], bonded a polyacrylamide layer on non-porous silica particles of 700 nm size packed in a 2.1-µm (internal diameter) ID column. With this material they obtained baseline separation of the five proteoforms of ribonuclease B, lowering the amount of TFA to 0.05% and adding 0.5% formic acid (FA). However, only the use of polymeric materials that are not based on silica, but, for example, exclusively on polyacrylamide, can fully exclude ion-exchange interaction with silanols. To date, no fully organic material for HILIC of intact proteins has been reported.

In this study, we set out to synthesize and optimize an acrylamide-based monolithic stationary phase for protein separations in HILIC. We aimed to explore the effects of varying the reaction mixture (monomer, crosslinker and porogens) and to characterize the different capillary columns in terms of permeability, hydrophilicity, morphology and porosity. Our aim was to obtain efficient columns for HILIC separations of intact proteins and proteoforms, which could be operated with very low concentrations of TFA as ion-pair reagent, so as to greatly enhance the sensitivity of MS detection in comparison with capillary columns packed with commercial silica-based amide stationary phases.

EXPERIMENTAL SECTION

MATERIALS

Acrylamide (A, electrophoresis grade, 99%), *N,N'*-methylenebisacrylamide (MbA, 99%), 3-(trimethoxysilyl)propyl methacrylate (γ-MAPS, 98%), 2,2'-azobisisobutyronitrile (AIBN, 98%), 1-octanol (OctOH, 99%), dimethyl sulfoxide (DMSO >99.9%), toluene, sodium hydroxide (NaOH), lysozyme from chicken egg white (Lys), carbonic anhydrase from bovine heart (CA, >90%), myoglobine from equine heart (Myo, >90%), cytochrome C (CC), bovine serum albumin (BSA), ribonuclease A from bovine pancreas (RnA), ribonuclease B from bovine pancreas (RnB, ≥80%), thyroglobulin (TG), transferrin from human serum, (Tf), cytosine (Cyt), trifluoroacetic acid (TFA, ≥99%), formic acid (FA, analytical grade >98%) were purchased from Sigma Aldrich (St. Louis, Missouri, United States). Methanol (MeOH), acetonitrile (ACN) were purchased from Biosolve (Valkenswaard, The Netherlands). Hydrochloric acid 37% (HCl) were obtained from Acros (Geel, Belgium). Milli-Q water (18.2 MΩcm) was produced by a Sartorius Arium 611UV Ultrapure Water System (Göttingen, Germany). The capillary (0.20 mm ID, 0.36 mm OD) was purchased from CMScientific (Silsden, UK). Glass tube lined (0.80 mm ID x 300 mm) was purchased from VICI (Valco Instrument Company Inc, TX)

PREPARATION OF POLY(ACRYLAMIDE-CO-N,N'-METHYLENEBISACRYLAMIDE) MONOLITHIC COLUMNS

Monolithic capillary columns were optimized for intact proteins separations. Prior the synthesis, in order to attach covalently the monolith to the inner wall surface, the fused-silica capillary was etched using NaOH and HCl and subsequently silanized using a 20% (v/v) γ-MAPS solution in toluene as described by Courtois *et al*.[30] Thereafter, the capillary was flushed with toluene and dried with nitrogen.

Several acrylamide-based monolithic capillary columns were synthesized starting from polymerization conditions similar to the procedure described by Fréchet *et al*[10], using the recipes in Table 1. The most difficult part consisted of dissolving completely the monomer and the crosslinker in the porogens. In order to solubilize the monomers, the MbA was added to the porogens and sonicated for 1h at a temperature between 30 and 40°C. Once the crosslinker was dissolved we added the monomer and kept sonicating for 45 min at the same temperature. At last, the AIBN (1% w/w respect to the monomers) was added and the mixture was vortexed. Subsequently, the silanized capillaries were filled with the polymerization mixture, and the ends were closed using rubber pieces. Polymerization took place for 24 h at 60 °C in a thermostated glass tube. Finally, the monolithic capillary columns were thoroughly flushed with MeOH.

Table 1. Monomer and porogen composition of the polymerization mixtures used to make the different acrylamide-based columns (the abbreviations of monomers and porogens are reported in the material and methods). All the % are as w/w.

Column	A%	MbA%	OctOH%	DMSO%	DMF%
A50	12.5	12.5	21.5	53.5	-
A55	13.75	11.25	21.5	53.5	-
A60	15	10	21.5	53.5	-
A65	16.25	8.75	21.5	53.5	-
13DMF	12.5	12.5	21.5	46.8	6.69
25DMF	12.5	12.5	21.5	40.1	13.38
37DMF	12.5	12.5	21.5	33.44	20.06
50DMF	12.5	12.5	21.5	26.75	26.75

An attempt of scaling-up the column dimensions was made in a glass lined tubing of 0.8 µm ID (150 mm length). The tubing was silanized, vinylized and polymerized as described before. The polymerization mixture used was the A55. No further optimization has been performed.

PREPARATION OF PACKED CAPILLARY COLUMNS

The columns were packed by preparing a slurry of 0.1 g/mL particles using methanol as packing solvent. The slurry was inserted in an empty column (4.6 mm × 50 mm) with one end drilled to be able to connect the capillary. The capillary was inserted 5 mm inside the packing column. A flow of 0.1 mL/min of the packing solvent was set. The

column was kept under flow for 30 min after the packing was complete. The slurry left was collected and the packed column was removed.

INSTRUMENTS AND CONDITIONS

SEM experiments. Scanning electron microscopy (SEM) images of cross-sections of the monoliths were recorded on an FEI Verios 460 instrument (Thermo Fisher Scientific, Eindhoven, The Netherlands) equipped with an Everhart-Thornley detector (EDT) using a 2-kV electron beam. The samples were sputter-coated with a 15-nm gold layer on top of a 5-nm layer of Palladium.

Permeability calculations. Permeability and hydrophilicity of the monolithic stationary phases were evaluated using a M-Class Acquity UPLC system (Waters, Milford, MA, USA), equipped with a binary solvent manager, a thermostated autosampler (1 µL sample loop) and a dual-wavelength UV-vis (TUV) detector with a 100 nL flow-cell. The permeability was determined flushing MeOH in the acrylamide-based monolithic columns at various flow rates between 0.5 and 3 µL/min and using the Darcy's law:

$$K_f = \frac{F_m \eta L}{\Delta P \pi r^2} \quad (1)$$

Where F_m is the flow rate of the solvent, η is the dynamic viscosity of the solvent, L is the length of the monolith, ΔP is the pressure drop across the monolithic column, and r is the radius of the capillary.

Hydrophilicity test. The hydrophilicity of the polymer monoliths was evaluated through the injection of 0.1 mg/mL cytosine sample at different mobile phases composition. The sample was diluted in ACN and MilliQ water, using percentages matching the mobile phase composition. The separations were performed isocratically, at room temperature (22 °C), with MilliQ water as mobile phase A and ACN as mobile phase B, both containing 0.1% and 0.005% (v/v) of TFA at a flow rate 2 µL/min.

Evaluation of monolith performance. Separations of intact proteins were performed on a UltiMate RSLCnano system (Thermo Fisher Scientific, Breda, The Netherlands) equipped with an autosampler (5 µL loop), thermo-controlled column compartment with ten ports, two-position valve and loading pump system (NCS-3500RS), and UV-vis detector (VWD-3400RS). As a trap-column, 20 × 0.3 mm ID C4, 5 µm, 300 Å (Thermo Fisher Scientific) was used to inject samples from water based solution, using a setup similar to what was described by Gargano *et al*[31].

Each reference protein was diluted in a solution of MilliQ: ACN = 95: 5 with the 0.1% TFA. The sample was loaded on the trap-column at 20 µL/min using the loading pump for 5 min with a mobile phase (A) of 2% ACN in water with 0.1% TFA. The valve was switched after 3 min from the beginning of the method.

Three washing cycles consisted of fast linear gradients from 20 to 80% and back to 20% of B (2% of MilliQ in ACN) in 2 min were added at the end of every separation, in order to avoid carryover. Further information about the method can be found in the figure captions.

The efficiency of the columns was assessed calculating the peak capacity (n_c) using the following equation (2):

$$n_C = \frac{t_G}{1.7 \times w_{0.5}} + 1 \quad (2)$$

Where t_G is the gradient time, while $w_{0.5}$ is the peak width at half-height.

The asymmetry of the peaks (A_S) was calculated through the Chromeleon software (Thermo Fisher scientific) according to the following equation (3):

$$A_S = \frac{RW_{5\%} + LW_{5\%}}{2 \times LW_{5\%}} \quad (3)$$

Where $RW_{5\%}$ and $LW_{5\%}$ are right and left peak width at 5% of the peak height, respectively.

The resolution for the separation of the five RnB proteoforms was calculated using the peak-valley ratio (P) equation (4) suggested by Christophe[32]:

$$P_{v,n} = 1 - v/h_n \quad (4)$$

Where v is the intensity of the valley between two peaks, and h_n is the intensity of the peak taken into consideration.

A separation of a protein mixture was performed also in the 0.8 µm ID monolithic column with the Waters system. Further information about the chromatographic conditions and a protein separation (Figure S7) can be found in the SI.

HILIC-HRMS conditions. A Q-Exactive Plus Biopharma (Thermo Fisher, Bremen, DE) instrument was operated positive-ion mode, using steel based emitters, a nano ESI source at a voltage of 2 kV, transfer capillary temperature of 300°C and S-lens of RF 70.

The analyzed samples consisted of a 0.5 mg/mL solution of four proteins such as CC, CA, BSA and Tf and a solution 0.5 mg/mL of RnB. The reference proteins were diluted in 10% ACN in water. The volume injected are 0.5 µL for the protein mixture and 1 µL for the RnB sample.

Acquisition parameters for the protein mix: m/z range, 400 - 6000 m/z; resolution @200 m/z, 17500; 10 microscans; max IT, 200 ms, AGC, 1e6, in source CID, 20 eV; HMR activated (trapping gas 1.2).

Acquisition parameters for RnB: m/z range 400 – 3000 m/z; resolution, 14000; 4 microscans; max IT 200 ms; AGC 1e6, in source CID 20 eV, intact protein mode activated (trapping gas 0.2).
Total-ion current (TIC) and extracted-ion current (EIC) chromatograms and deconvoluted RnB masses were obtained using the Freestyle software (Thermo Fisher scientific). While deconvoluted masses of the other proteins were obtained using UniDec[33], tuning several parameters. Charge range, mass range and sample mass every were 1-30, 12000-13000 Da, 5 Da for CC, 1-50, 28000-29500 Da, 1.0 Da for CA, 1-50, 66000-68000, 1.0 Da For BSA, 1-80, 79000-80000 Da, 1.0 Da for Tf respectively.
Extracted-ion current chromatograms of the RnB (140000 Resolution) were obtained from 5 charge states (m/z 2129.3990, 1863.3501, 1656.4233, 1490.8819, 1242.5694) for RnB1, 5 charge states (m/z 2152.5490, 1883.6070, 1674.4294, 1507.1871, 1256.0739) for RnB2, 5 charge states (m/z 2175.6998, 1903.8632, 1692.4352, 1269.5785, 1523.2921) for RnB3, 5 charge states (m/z 2198.8515, 1924.1203, 1710.5526, 1539.5978, 1283.1666) for RnB4 and 5 charge state (m/z 2222.0021, 1944.5020, 1728.5585, 1555.7030, 1296.6706) for RnB5 with an extraction window of 10 ppm. A smoothing Gaussian 7 was applied to all the chromatograms.

RESULTS AND DISCUSSION

FABRICATION AND OPTIMIZATION OF THE MONOLITHIC STATIONARY PHASES

The composition of the polymerization mixture strongly affects the morphology and efficiency of organic monoliths. Based on the study made by Xie *et al*[10], we selected DMSO and OctOH as porogen system for our polymerization. While DMSO is capable to dissolve the monomers (good solvent), alone it cannot provide pores sufficiently large. Therefore OctOH is used as “poor solvent” to promote the development of flow-through pores.
In our experiments, we first used the ratio A: MbA = 70: 30 described by Xie[10] and polymerized the reaction mixture using DMSO/ OctOH and in 200 µm ID capillaries using thermal polymerization. The columns could be flushed using methanol however the material would dissolve when exposed to high amount of water. Therefore, to obtain more rigid and water resistant polymers we used a higher percentage of crosslinker (A: MbA = 50: 50), as described in Table 1.
To guarantee an acceptable back pressure and a less dense polymer structure, the overall amount of porogens employed (from 70 of the original mixture to 75% w/w) was increased. Using these experimental conditions, we obtained polymer monoliths that could withstand pressures over 400 bars (maximum pressure at which we operated the columns) in organic and aqueous conditions. Next we prepared a series of acrylamide-based monolithic columns studying the influence of different monomer and porogen solvent composition, testing in particular the effect of the A to MbA ratio and the type of porogen system (using DMF as ternary solvent). The composition of the polymerization mixtures used is reported in Table 1.

CHARACTERIZATION OF POLYACRYLAMIDE MONOLITHIC MATERIALS

To characterize the polyacrylamide based polymerization mixtures, we prepared capillary columns (in triplicate per polymerization mixture) and tested their permeability. Selected columns with different permeability were analyzed using scanning electron microscopy to ensure the binding to the capillary wall and inspect the different globule features.

Permeability. The columns were tested before and after chromatographic separations and a change of permeability values as well as a shift of the retention times in the separations was noticed for some of the columns: A60, A65, 13DMF and 50DMF. The permeability values of these columns are reported in SI (see Figure S1). We suggest that respectively, the reduced amount of crosslinker (for the A60 and A65) and early phase separation for the ternary porogens polymerization mixtures (13DMF and 50DMF) can result in unstable monolithic structures.
According to the Darcy’s law, the calculated permeability for the A50 columns, obtained from a 50/50 A/MbA mixture resulted in a permeability of $4.90 \cdot 10^{-14}$ m^2. Increasing the amount of crosslinker up to 55% lead to a small decrease in permeability ($K_f = 2.92 \cdot 10^{-14}$). The lower permeability, similar to the ones of 2.7 µm ID core-shell particles ($K_f = 1.42 \cdot 10^{-14}$ m^2)[34], is justified by an earlier phase separation during the polymerization induced by a higher amount of MbA employed. As far as it concerns the 25DMF columns, the introduction of a third non-polar porogen (DMF) in the polymerization mixture induces an earlier phase separation compared to the binary porogen mixtures that leads to the formation of smaller pores. However the permeability of the material decrease from 13 to 25% DMF and increase when increasing the DMF content to 37 and 50%, with the lower permeability being for 25% DMF ($K_f = 7.64 \cdot 10^{-15}$). The latter is in the same order of magnitude of the 1.7 µm ID fully porous particles ($K_f = 5.21 \cdot 10^{-15}$ m^2)[34].

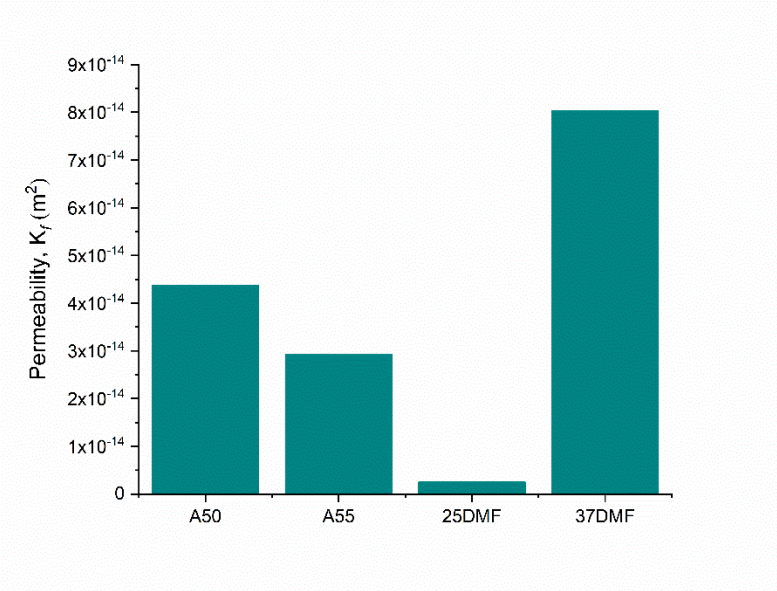

Figure 1. Permeability values of the acrylamide-based monolithic stationary phases.

Scanning Electron Microscopy. SEM images were used to confirm the attachment to the capillary walls, the monolith homogeneity (see Figure S2a-b) and to evaluate the influence of the different porogen as well as the different amount of crosslinker used. We used this approach to analyze columns 25DMF, A50 and A55. All the monolithic stationary phases had a homogeneous micro-globular structure and a good attachment to the inner wall of the capillary. Figure 2 shows that the monolithic stationary phase in which the 25% of the DMSO was substituted with DMF (2A) creates smaller globules compared to the A50 (2B) (approximately xx compared to xx). Similarly, Figure 2C shows a small reduction of the globule size when increasing percentage of crosslinker as demonstrated by Viklund *et al*.[35]

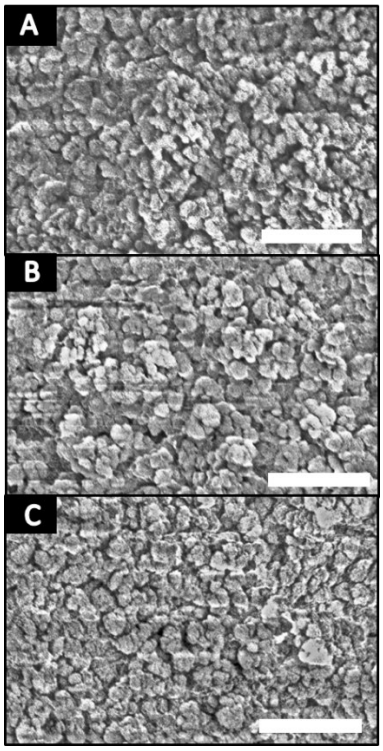

Figure 2. SEM images of cross-sections of three different acrylamide-based monolithic capillary columns. A) 25DMF, B) A50, C) A55. Scale bars 10 µm.

Hydrophilicity of the stationary phases: retention of nucleobases. An important characteristic of HILIC stationary phases is their hydrophilicity. The water intake of a polar stationary phase highly influences the retention mechanism and the chromatographic separation. To demonstrate that our monolithic columns show a typical HILIC

behavior we used A55 to perform isocratic separations at different water percentages of a polar compounds: Cyt (see Figure S3). From this analysis it is clear that the stationary phase has mostly hydrophilic interaction behavior (retention with ACN % above 60%) and little to no RPLC retention (below 40% ACN), proving the hydrophilicity of the material.[36]

CHROMATOGRAPHIC PERFORMANCE OF POLYACRYLAMIDE MONOLITHS

Polyacrylamide monolith for the separation of intact proteins.

In order to find a good compromise between analysis time and efficiency, we tested a wide range of flow rates (from 1 µL/min to 5 µL/min) on a A55 capillary column maintaining the gradient volume constant (70 µL, see Table S2). The highest peak capacity (n_c = 106) was achieved at 1 µL/min in a 70 min gradient. However in order to reduce the analysis time a flow rate of 2 µL/min was chosen and further used in our study.

To test the different column materials described in table 1 we applied the same gradients (see experimental conditions) at 2 µL/min and 60°C. The columns were used to separate a mixture of reference proteins: Myo, Lys, CA and RNA. These proteins have different MW (13 to 30 kDa), pI (6.4 to 9.32) and limited proteoforms that could lead to peak broadening in UV due to partial resolution. In addition, we used RnB as sample representative of glycoprotein separations. The results of this study are reported in Figure 3, S4 and S5.

The peak capacities for the protein mixture vary between 28 of 13DMF to 51 of A55 (see Table S5). The columns present sufficient separation capacity for the RnB glycoforms. The five peaks are well-recognizable in most of the columns (see Figure S5) and partially resolved (see Table S5).

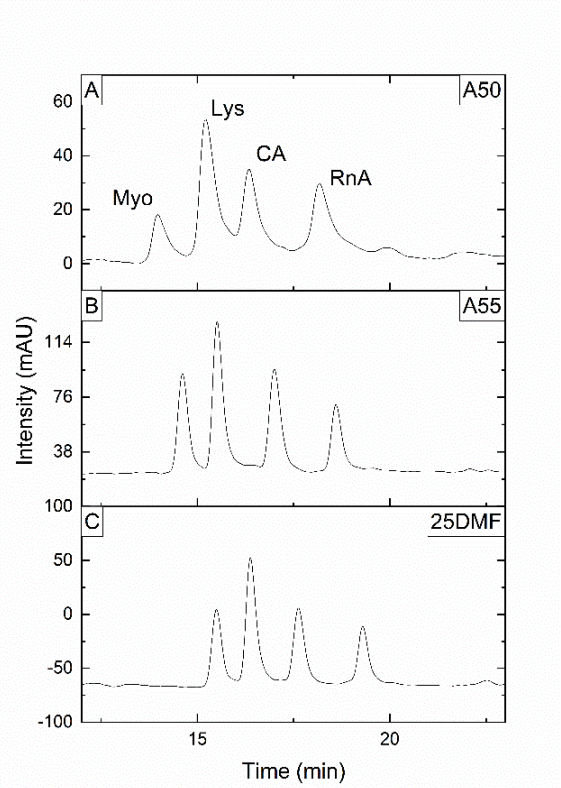

Figure 3. HILIC separation of intact proteins (A-C) in the 3 capillary columns A50, A55, 25DMF. The analysis was performed using a gradient from 90 to 85% (v/v) of B in 1 min and then down to 55% in 25 min at a flow rate of 2 µL/min. The analysis was carried at 60°C and UV wavelength monitored was 214 nm. The chromatograms of all the columns in table 1 is in Figure S4 of the SI.

Figure 3 shows the separation of four proteins using the monolithic stationary phases that give the best results: A50, A55 and 25 DMF. Good peak shape (with minor tailing, with asymmetry between 1.13 and 1.47) and average peak capacity (36 and 51) are achieved in these columns. The lower permeability and higher retention times of the 25DMF columns compared to the A55 (see Table S3) suggest an increased surface area in this column. Similar peak-valley ratio values were found for the A55 and 25DMF (see Table S6). All the three polymerization mixtures presented good batch-to-batch repeatability (variation of rention time and peak capacity < 5%).

Even though the A55 and 25DMF gave similar results, we chose A55 to continue our study because of its higher repeatability, higher permeability and its potential of allowing for the polymerization of longer columns.

Comparison of protein separations in polyacrylamide monoliths vs silica particles at different % of TFA. Next, we compared the performance of our polyacrylamide column A55 and a packed capillary column, to assess if our new developed material can be used with lower amount of TFA. The packed column was prepared using 2.7 µm ID core-shell amide silica particles, used in our previous work[22,25,28]. The two HILIC columns were compared using different concentrations of TFA (0.1, 0.5 and 0.025 and 0.005% TFA) in the mobile phase (Figure 5). To evaluate the performance of the two columns we used a protein mixture, including proteins of higher molecular weight, including CC, CA, BSA and Tf and the glycoprotein RnB. These proteins cover a wide range of molecular weight (12 to 80 kDa) and isoelectric point (5.60 to 9.59).

We applied the same gradient (83-65% of B in 26 min) using 0.1% (v/v) TFA to the separation of the protein mix in both columns. Interestingly, the peak capacity of the two columns is similar (32 vs 31) but the selectivity is different. In the silica column, the protein mix is not fully separated and CA and BSA co-elute while in the polyacrylamide column the 4 peaks are baseline separated (Figure 5a and Table S6). The separation of RnB under gradient conditions (76-62% of B in 26 min) leads to the partial separation of the 5 glycoforms in both columns with similar results in terms of peak-valley ratio values (see Table S7). Comparing the retention of the proteins between the two columns, the proteins elute at a higher percentage of B (ca. 2% more ACN) in the monolithic column possibly due to the lower surface area of this support (Table S6-7).

The same gradient used for 0.1% TFA was used for separations of the protein mixture at 0.005% TFA (Figure 5B). In the case of the polyacrylamide column, the retention reduced between separations at high (0.1%) and low concentration (0.005%) of TFA, with a minor reduction of peak capacity (31 vs 22). A possible explaination for the change in retention is the increased hydrophilic character of the water phase due to the decrease (20x) of the fluorinated ion-pairing reagent in the mobile phase. In the case of the silica-based column, one of the protein (Tf) could not elute from the column (even when increasing the water content up to 90%) and the separation significantly worsen (peak capacity of 12) with only two peaks present in the chromatogram having significant tailing. We speculate that the increase of ion-exchange interaction due to the decrease of ion-pairing reagent in the mobile phase is at responsible for this phenomena. In-depth analysis of the effect of different ion-pair agents and their concentrations is currently ongoing and will be discussed separately.

For the separation of RnB we broaded the gradient in the case of the polyacrylamide column (83-63% B in 26 min), while a shallower gradient (75-68% B in 26 min) was used in the silica-based column. At a lower concentration of ion-pairing reagent, the RnB elutes at 75% and 73% of B in the polyacrylamide and particles column, respectively. Lower percentages (71 and 69) are required when the concentration of TFA is 0.1% (v/v).

Despite the optimization, at 0.005% (v/v) TFA, the monolithic column outperforms the silica-based column, as confirmed by the peak-valley ratio values in Table S8 (report key values).

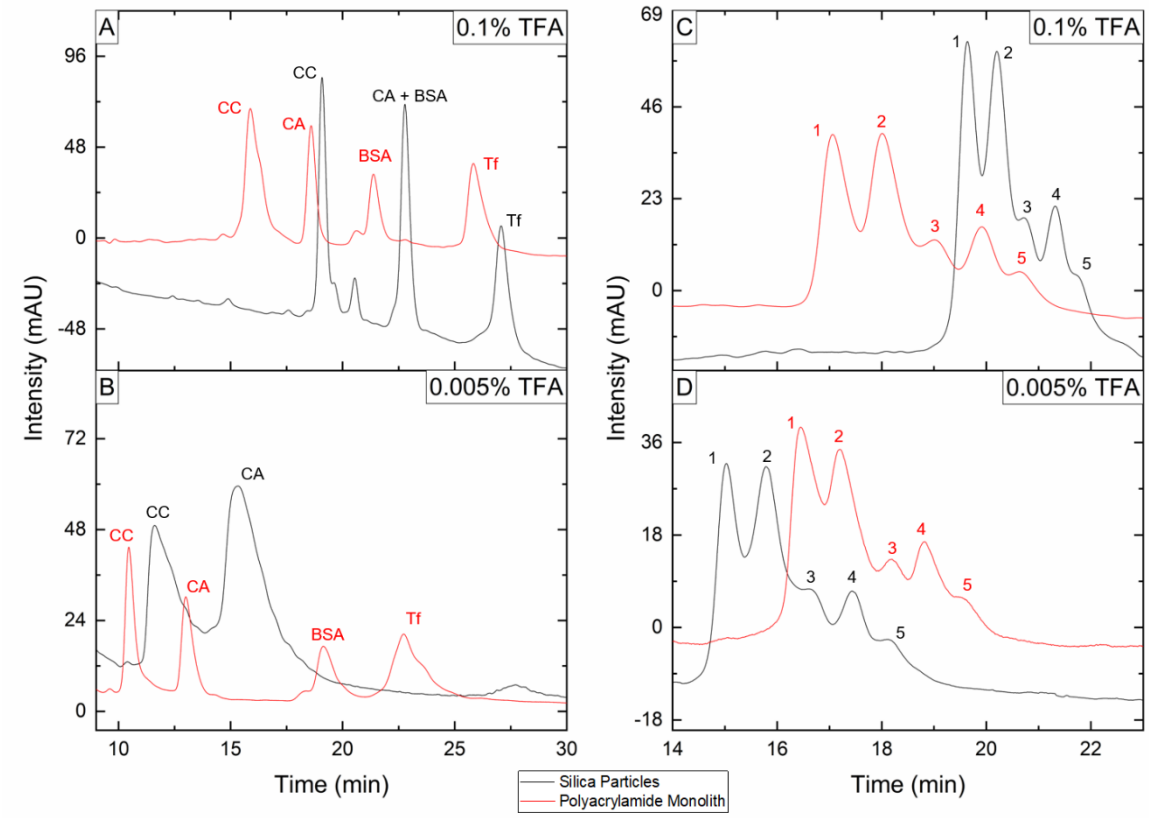

Figure 5. Comparison of HILIC separations with 0.1% (v/v) TFA (A-C) and with 0.005% (v/v) TFA (B-D) in the mobile phases. A-B) HILIC separation of 4 intact proteins on the particles column (black) and on the monolithic column (red). The analyses were performed using a gradient from 94 to 83% (v/v) of B in 1 min and then down to 65% in 26 min. Protein elution order: CC, CA, BSA, Tf. C) HILIC separation of glycoforms of RnB on the particles column (black) and on the monolithic column (red). The analyses were performed using a gradient from 94 to 76% (v/v) of B in 1 min and then down to 62% in 26 min. D) HILIC separation of glycoforms of RnB on the particles column (black) and on the monolithic column (red). D-black) The analyses was performed using a gradient from 94 to 75% (v/v) of B in 1 min and then down to 68% in 26 min. D-red) The analyses was performed using a gradient from 94 to 82% (v/v) of B in 1 min and then down to 63% in 26 min All the analyses were carried at 45°C using a flow rate of 2 µL/min and the monitored UV wavelength was 214 nm.

Polyacrylamide columns for HILIC-HRMS with low TFA content. High resolution mass spectrometry (HRMS) is an effective tool to characterize proteoforms of proteins as these can be clearly identified with mass shift and further confirmed by fragmentation experiments[37,38]. HILIC mobile phases are rich in ACN and this typically favours desolvation. However in the case of HILIC of intact glycoproteins, the presence TFA (0.1% v/v, 13 mM), needed to ensure good glycoforms resolution, causes signal suppression and protein-TFA adducts. To reduce adduct formation high activation energies have to be used[25], however under these conditions some proteins may undergo fragmentation. For this reason, in other research we have tested post-column solutions to decrease the adducts formations during HILIC-MS. [31,39]

Reducing the content of TFA in the mobile phase should reduce adduct formation in HILIC-MS. To investigate this, we tested our polyacrylamide columns using mobile phases with 0.1% TFA, 0.005%TFA and 0.1% FA and 0.005% TFA. We applied the same gradient (87-70% of B in 35 min) for the separations at lower concentration of TFA (0.005%) with and without FA.

Figure 6. TIC (a,c) and EIC (b,d) chromatograms obtained from a HILIC-MS method using a, b) 0.1% (v/v) TFA, c, d) 0.005% (v/v) TFA + 0.1% (v/v) FA. A) The analyses was performed using a gradient from 94 to 83% (v/v) of B in 2 min and then down to 67% in 35 min. B-D) The analyses were performed using a gradient from 94 to 87% (v/v) of B in 2 min and then down to 70% in 35 min. All the analyses were carried at 45°C using a flow rate of 1.5 µL/min. The EIC were performed summing the intensity of different charge state for CC (883.8 ,951.7,1030.9, 1124.4, 1236.8,1374.1,1545.7, 1766.2, 2060.5 m/z), CA (937.3, 968.4,1001.9,1037.6,1076.6,1117.3,1161.9,1210.4,1262.8,1320.3,1383.0,1452.3,1528.5,1613.4,1708.2 m/z), BSA (1278.5, 1303.5, 1329.6, 1356.6, 1384.9, 1414.4, 1445.1, 1477.2, 1510.7, 1545.8, 1582.0, 1621.2, 1664.5,1704.2 m/z) and Tf (2040.8, 2094.5, 2151.1, 2210.8, 2273.9, 2340.8, 2411.7, 2487.0, 2567.2, 2652.7, 2744.2 m/z) all the EIC are +/- 0.2 m/z

Figure 6 shows TIC and EIC chromatograms recorded using the methods described in the captions. The EIC chromatograms of the separation performed at higher TFA concentration show lower intensity and lower area compared to the separation carried out with lower amout of TFA.
At high concentration of TFA, the efficiency of the column is indeed higher than the separation carried at lower percentage of TFA (peak capacity, 42 vs 15). The latter shows broader peak shapes that result in a partial lost of selectivity.
Neverthless, when adding FA to the mobile phase with low TFA content, the separation performances increase (peak capacity 40). Sharper peak shapes are obtained and the selectivity is restored. Moreover, FA does not influence MS spectra since it does not create adducts.

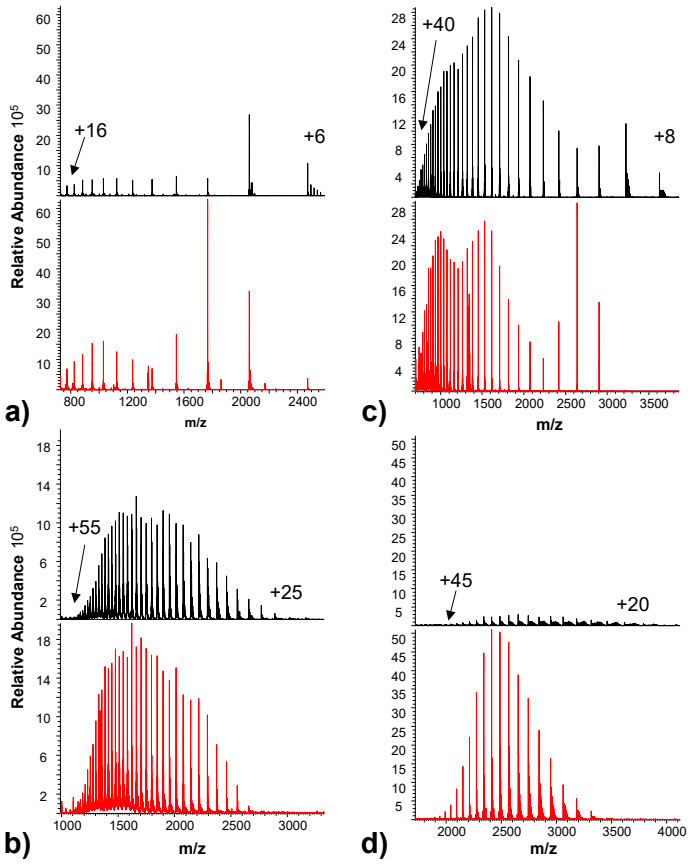

Figure 7. Average spectrum from the chromatographic peak of a) CC, b) CA, c) BSA, d) Tf obtained from the HILIC-MS method reported in Figure 6. 0.1% (v/v) TFA (black trace) and 0.005% (v/v) TFA + 0.1% (v/v) FA (red trace). The numbers on the mass spectra indicate the charge state interval.

Figure 7 shows average spectra of the 4 proteins obtained from the HILIC-MS separations using different concentrations of TFA. The black traces indicate the protein spectra carried using a mobile phases with 0.1% v/v TFA, while the red trace are for the separation at lower concentration of TFA. There is a shift to higher charge states in the separations with 0.005% TFA.
The intensity of the red traces is higher than the black traces. This increase in sensitivity is mostly visible in the spectra of proteins with higher molecular weight. In fact, the normalization level of the Tf in the red trace is almost one order of magnitude higher than the one in the black trace. The number of TFA-protein adducts is bigger compares to the small protein that have less interaction sites.
Due to the formation of a lower amount of adducts, a shift to higher charge states (lower m/z) is noticed when using 0.005% v/v TFA in the mobile phase. A lower amount of TFA induces a broader charge distribution and shift of the most intense charge state. The increased multiple charging permits a more accurate mass measurement, allowing the use of less sophisticated MS analyzers, and structural characterization of the proteins by tandem mass spectrometry due to its efficient fragmentation.

CONCLUSIONS

Several acrylamide-based monolithic stationary phases with different porosity were successfully created within 200 µm ID capillary using thermal polymerization. From SEM pictures, the micro-globular structure resulted homogenous, but the monolithic stationary phases prepared with the addition of DMF as a third porogen show

smaller pores. Through the separation of 4 intact proteins, we obtained a peak capacity of 51 and 50, respectively for the A55 and 25DMF. Also in the separation of the five proteoforms of RnB, the two columns shows similar performances. We selected the A55 for further experiments due to its higher permeability and the possibilities of creating longer columns.
At higher concentration of TFA (0.1% v/v), the A55 shows more selectivity but similar peak capacity compared to a packed column (amide). Nonetheless, at lower concentration of TFA, there is no loss of selectivity and the peak capacity goes from 29 to 25 for the monolithic column. On the other side, the amide column shows broader peak shapes and a change of selectivity, especially for the glycoforms of the RnB.
The coupling with MS showed how the reduction of TFA in the mobile phase allows to enhance the sensitivity of one order of magnitude for the bigger proteins (e.g. Tf). The lost in chromatographic efficiency can be compensated by the addition of 0.1% (v/v) FA, bringing the peak capacity from 21 to 50. Moreover, from the spectra and the deconvoluted spectra, it is clear that the major advantage of using this stationary phase is for the big proteins as a lower amount of TFA is translated in a lower amount of TFA-protein adducts.

- Future perspective, The chemistry of these materials can be used as support for making monolithic columns with low hydrophobicity such as in ion-exchange, affinity chromatography and size exclusion.

SUPPORTING INFORMATION

The supporting information is available free of charge on the ACS Publication website at DOI:

AUTHOR INFORMATION
Corresponding Authors
E-mail: m.passamonti@uva.nl; Mailing Address: Marta Passamonti, Faculty of Science, Van ‘t Hoff Institute of Molecular Science (HIMS), P.O. Box 94157, 1090GD Amsterdam, The Netherlands.
ORCID 000-0002-6691-4054
E-mail: a.gargano@uva.nl; Mailing Address: Analytical Chemistry, Center for Analytical Sciences Amsterdam, Science Park 904, Building C2, room 258, Universiteit van Amsterdam, 1098 XH Amsterdam, The Netherlands
ORCID 0000-0003-3361-7341

ACKNOWLEDGEMENTS

The STAMP project is funded under Horizon 2020-Excellent Science-European Research Council (ERC), Project 694151. The sole responsibility of this publication lies with the authors. The European Union is not responsible for any use that may be made of the information contained therein.

REFERENCES

(1) Mair, D. A.; Geiger, E.; Pisano, A. P.; Fr?chet, J. M. J.; Svec, F. *Lab Chip* **2006**, *6* (10), 1346.
(2) Krenkova, J.; Foret, F. *Anal. Bioanal. Chem.* **2013**, *405* (7), 2175–2183.
(3) Wouters, B.; Dapic, I.; Valkenburg, T. S. E.; Wouters, S.; Niezen, L.; Eeltink, S.; Corthals, G. L.; Schoenmakers, P. J. *J. Chromatogr. A* **2017**, *1491*, 36–42.
(4) Passamonti, M.; Bremer, I. L.; Nawada, S. H.; Currivan, S. A.; Gargano, A. F. G.; Schoenmakers, P. J. *Anal. Chem.* **2020**, *92* (3), 2589–2596.
(5) Currivan, S.; Connolly, D.; Gillespie, E.; Paull, B. *J. Sep. Sci.* **2010**, *33* (4–5), 484–492.
(6) Hjertén, S.; Yi-Ming Li, Y.; Liao, J.-L.; Mohammad, J.; Nakazato, K.; Pettersson, G. *Nature* **1992**, *356* (6372), 810–811.
(7) Hjertén, S.; Mohammad, J.; Nakazato, K. *J. Chromatogr. A* **1993**, *646* (1), 121–128.
(8) Zeng, C. M.; Liao, J. L.; Nakazato, K.; Hjertén, S. *J. Chromatogr. A* **1996**, *753* (2), 227–234.
(9) Hoegger, D.; Freitag, R. *Electrophoresis* **2003**, *24* (17), 2958–2972.
(10) Xie, S.; Svec, F.; Fréchet, J. M. J. *J. Polym. Sci. Part A Polym. Chem.* **1997**, *35* (6), 1013–1021.
(11) Jiang, H.; Yuan, H.; Qu, Y.; Liang, Y.; Jiang, B.; Wu, Q.; Deng, N.; Liang, Z.; Zhang, L.; Zhang, Y. *Talanta* **2016**, *146*, 225–230.
(12) Hoegger, D.; Freitag, R. *Electrophoresis* **2003**, *24* (17), 2958–2972.
(13) Lindner, H.; Sarg, B.; Meraner, C.; Helliger, W. *J. Chromatogr. A* **1996**, *743* (1), 137–144.
(14) Lindner, H.; Sarg, B.; Helliger, W. *J. Chromatogr. A* **1997**, *782* (1), 55–62.
(15) Tian, Z.; Tolić, N.; Zhao, R.; Moore, R. J.; Hengel, S. M.; Robinson, E. W.; Stenoien, D. L.; Wu, S.; Smith, R. D.; Paša-Tolić, L.; Toli, N.; Zhao, R.; Moore, R. J.; Hengel, S. M.; Robinson, E. W.; Stenoien, D. L.; Wu, S.; Smith, R. D.; Pa, L. *Genome Biol.* **2012**, *13* (10), R86.
(16) Carroll, J.; Fearnley, I. M.; Walker, J. E. *Proc. Natl. Acad. Sci. U. S. A.* **2006**, *103* (44), 16170–16175.
(17) Tetaz, T.; Detzner, S.; Friedlein, A.; Molitor, B.; Mary, J.; Peek, Z. *J. Chromatogr. A* **2011**, *1218* (35), 5892–5896.
(18) Zhang, Z.; Wu, Z.; Wirth, M. J. *J. Chromatogr. A* **2013**, *1301*, 156–161.
(19) Pedrali, A.; Tengattini, S.; Marrubini, G.; Bavaro, T.; Hemström, P.; Massolini, G.; Terreni, M.; Temporini, C. *Molecules* **2014**, *19* (7), 9070–9088.
(20) Lauber, M. A.; Yu, Y. Q.; Brousmiche, D. W.; Hua, Z.; Koza, S. M.; Magnelli, P.; Guthrie, E.; Taron, C. H.; Fountain, K. J. *Anal. Chem.* **2015**, *87* (10), 5401–5409.
(21) Periat, A.; Fekete, S.; Cusumano, A.; Veuthey, J.-L. L.; Beck, A.; Lauber, M.; Guillarme, D. *J. Chromatogr. A* **2016**, *1448*, 81–92.
(22) Tengattini, S.; Domínguez-Vega, E.; Temporini, C.; Bavaro, T.; Rinaldi, F.; Piubelli, L.; Pollegioni, L.; Massolini, G.; Somsen, G. W. *Anal. Chim. Acta* **2017**, *981*, 94–105.
(23) D’Atri, V.; Fekete, S.; Stoll, D.; Lauber, M.; Beck, A.; Guillarme, D. *J. Chromatogr. B Anal. Technol. Biomed. Life Sci.*

2018, *1080* (January), 37–41.
(24) D'Atri, V.; Nováková, L.; Fekete, S.; Stoll, D.; Lauber, M.; Beck, A.; Guillarme, D. *Anal. Chem.* **2019**, *91* (1), 873–880.
(25) Domínguez-Vega, E.; Tengattini, S.; Peintner, C.; van Angeren, J.; Temporini, C.; Haselberg, R.; Massolini, G.; Somsen, G. W. *Talanta* **2018**, *184*.
(26) Liu, A. P.; Patel, S. K.; Xing, T.; Yan, Y.; Wang, S.; Li, N. *J. Pharm. Biomed. Anal.* **2020**, *189*, 113481.
(27) Gargano, A. F. G.; Schouten, O.; van Schaick, G.; Roca, L. S.; van den Berg-Verleg, J. H.; Haselberg, R.; Akeroyd, M.; Abello, N.; Somsen, G. W. *Anal. Chim. Acta* **2020**, *1109*, 69–77.
(28) Sénard, T.; Gargano, A. F. G.; Falck, D.; de Taeye, S. W.; Rispens, T.; Vidarsson, G.; Wuhrer, M.; Somsen, G. W.; Domínguez-Vega, E. *Front. Immunol.* **2020**, *11* (August), 1–13.
(29) Bobaly, B.; Beck, A.; Fekete, J.; Guillarme, D.; Fekete, S. *Talanta* **2015**, *136*, 60–67.
(30) Courtois, J.; Szumski, M.; Byström, E.; Iwasiewicz, A.; Shchukarev, A.; Irgum, K. *J. Sep. Sci.* **2006**, *29* (2), 324.
(31) Gargano, A. F. G.; Roca, L. S.; Fellers, R. T.; Bocxe, M.; Domínguez-Vega, E.; Somsen, G. W. *Anal. Chem.* **2018**, *90* (11), 6601–6609.
(32) Christophe, A. B. *Chromatographia* **1971**, *4* (10), 455–458.
(33) Marty, M. T.; Baldwin, A. J.; Marklund, E. G.; Hochberg, G. K. A.; Benesch, J. L. P.; Robinson, C. V. *Anal. Chem.* **2015**, *87* (8), 4370–4376.
(34) Cabooter, D.; Lestremau, F.; Lynen, F.; Sandra, P.; Desmet, G. *J. Chromatogr. A* **2008**, *1212* (1–2), 23–34.
(35) Viklund, C.; Svec, F.; Fréchet, J. M. J.; Irgum, K. *Chem. Mater.* **1996**, *8* (3), 744–750.
(36) Jandera, P.; Hájek, T.; Škeříková, V.; Soukup, J. *J. Sep. Sci.* **2010**, *33* (6–7), 841–852.
(37) Schachner, L. F.; Tran, D. P.; Lee, A. S.; McGee, J. P.; Jooss, K.; Durbin, K. R.; Seckler, H. S.; Adams, L.; Cline, E. N.; Melani, R. D.; Ives, A. N.; Soye, B. Des; Kelleher, N. L.; Patrie, S. M. *Int. J. Mass Spectrom.* **2021**, *465*, 116591.
(38) Toby, T. K.; Fornelli, L.; Kelleher, N. L. *Annu. Rev. Anal. Chem.* **2016**, *9* (1), 499–519.
(39) Wouters, S.; Eeltink, S.; Haselberg, R.; Somsen, G. W.; Gargano, A. F. G. *Anal. Bioanal. Chem.* **2021**.